Microstructure of α' martensites in Ti-V-Al alloys studied by high-resolution transmission electron microscopy

K. Sato[1], H. Matsumoto[1], A. Chiba[1], T. J. Konno[1]

[1]Institute for Materials Research, Tohoku University
2-1-1 Katahira, Aoba, Sendai, Miyagi 980-8577, Japan

Keywords: Ti-6Al-4V, TEM, Aberration correction, α'-Martensite, Stacking faults

Abstract

Atomic structures of hexagonal α' martensites in Ti-6mass%Al-4mass%V alloys have been studied by means of aberration corrected high-resolution transmission electron microscopy and electron diffraction. There observed differences in atomic structures of the $\{10\bar{1}1\}$-type twin boundaries of the α' martensites: stacking faults, a few atomic layers in width, was observed at the twin boundary for the as-quenched alloy after solution treatment at 1100°C (above the β transus), while the alloy solution treated at 950°C (below the β transus) showed a clear-cut twin boundary. The excellent ductility is observed in the latter alloy.

Introduction

Titanium alloys are suitable for aerospace, automobile and biomedical applications due to the high specific strength, low density, and good corrosion resistance [1-3]. Among the various types of Ti-alloy systems, Ti-6mass%Al-4mass%V (Ti-6Al-4V) alloys composed of α (hexagonal close-packed, hcp) and β (body-centered cubic, bcc) two-phases are widely used in various fields and much attention has been paid to the microstructure in relation to their excellent mechanical properties. The strengthening of the α+β two-phase alloy can be attributed to the perturbation of dislocation motion at the α/β interfaces [4]. In contrast to the two-phase Ti-alloys, low Young's moduli, high strength and excellent ductility have been realized by one of the authors in Ti-V-(Al or Sn) alloys with hexagonal α' martensites [5, 6]. Recent study has revealed that ductility of α'-type Ti-6Al-4V alloys is quite sensitive to the solution treatment temperature [7]. However, α' martensite is not in common use until now, and therefore, there is a few reports on microstructural control of the α'-type martensite alloys [8-10].

Here we report on the atomic structure of α' martensites in Ti-6mass%Al-4mass%V alloys studied by aberration corrected (AC) high-resolution transmission electron microscopy (HRTEM). In addition to highly improved spatial resolution, AC-HRTEM benefits from smaller defocus values under optimal defocus conditions due to small spherical aberration (C_s) values, which enables unambiguous identification of interface structures free from contrast delocalization.

Experimental Procedure

Ti-6mass%Al-4mass%V alloys were prepared by arc melting in an argon atmosphere using high purity Ti, V, and Al, followed by homogenization at 1150°C for 24h. The homogenized buttons were hot rolled at 850°C, followed by solution treatment at 950°C (below the β transus of 995°C) or 1100°C (above the β transus) for 1h in an evacuated quartz tube, and then quenched into ice water (STQ). These solution treatment temperatures are higher than the martensitic transformation starting temperature of approximately 900°C [11]. Chemical analysis for the STQ alloy showed nitrogen and oxygen contents of 0.0058mass% N and 0.123mass% O, respectively [10]. Phase identification was carried out by means of x-ray diffraction (XRD) using a

Panalytical X'pert MPD diffractometer with a Cu-Kα_1 radiation. Microstructures of these alloys were studied by using an FEI Titan 80-300 TEM operating at 300 kV with a field emission gun and a CEOS image corrector. The corrected spherical aberration (C_s) was smaller than 10μm. All HRTEM images were recorded by a 1k × 1k charge coupled device (CCD) camera. HRTEM images were simulated by using the MACTEMPAS software, which is based on the multislice method. Elemental analyses were carried out by using an energy dispersive x-ray spectrometer (EDS) attached to the TEM.

Results and Discussion

Figure 1a shows an HRTEM image of an as-quenched Ti-6Al-4V alloy after solution treatment at 1100°C, showing a thin twin band with thickness of 8nm. This twin is identified as $\{10\bar{1}1\}$-type twin formed by martensitic transformation. Actually, the $\{10\bar{1}1\}$ twin is typically observed in quenched Ti-V alloys with a hexagonal α' martensite structure [5, 11]. Stacking faults, a few atomic layers in width, can be seen clearly at the twin boundaries. It is considered that these stacking faults were formed at the quench, since the $\{10\bar{1}1\}$-type twin is characteristic of the martensitic transformation. Selected area electron diffraction (SAED) pattern, with a beam incidence of $[0\bar{1}\bar{1}1]_{\alpha'}$, shows weak streaks in the $[10\bar{1}\bar{1}]_{\alpha'}$ direction as well as extra reflections due to the twins as indicated by arrowheads. A magnified image of the twin boundary is shown in Fig.1c. As seen, there exist thin stacking faults at the twin boundary parallel to $\{10\bar{1}1\}$ atomic plane.

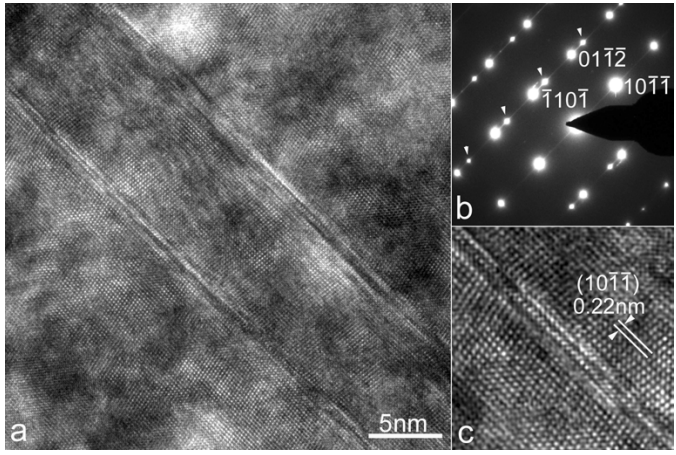

Figure 1. Microstructure of the as-quenched Ti-6Al-4V alloy after solution treatment at 1100°C. (a) HRTEM image of $\{10\bar{1}1\}$-type twin boundaries. (b) SAED pattern with the beam incidence of $[0\bar{1}\bar{1}1]_{\alpha'}$. Extra reflections due to the $\{10\bar{1}1\}$ twins are seen, as indicated by arrowheads. (c) A magnified image of the twin boundary. Stacking faults are clearly seen at the twin boundary.

Figure 2a shows another example of a thin twin plate observed in the as-quenched Ti-6Al-4V alloy after solution treatment at 1100°C. Here α' crystals termed as crystals 2 and 3 are connected by a $\{10\bar{1}1\}$-type twin, and crystals 3 and 4 are as well. Thus the α' crystal 3 is a thin twin plate with 6nm in width. At the twin boundary, stacking faults are seen. On the other hand, a thin β layer, 10nm in width, can be seen in addition to the thin $\{10\bar{1}1\}$ twin plate. The β layer is sandwiched by α' crystals 1 and 2. It is interesting that these crystals 1 and 2 have a same crystallographic orientation with the beam incidence of $[0\bar{1}\bar{1}1]_{\alpha'}$, and thus, the trace of the β layer is parallel to the $\{10\bar{1}\bar{1}\}_{\alpha'}$ plane. The orientation of each crystal can be confirmed by attached Fourier spectra. Note that the β layer contains significant lattice distortion at an area near the α'/β boundary. Fig.2g shows a magnified image of the boundary area of α'/β interface. The lattice distortion is seen inside the β phase region. It is presumed that the origin of the formation of such a thin β layer is related to a thin $\{10\bar{1}1\}$ twin plate formed by the martensitic transformation.

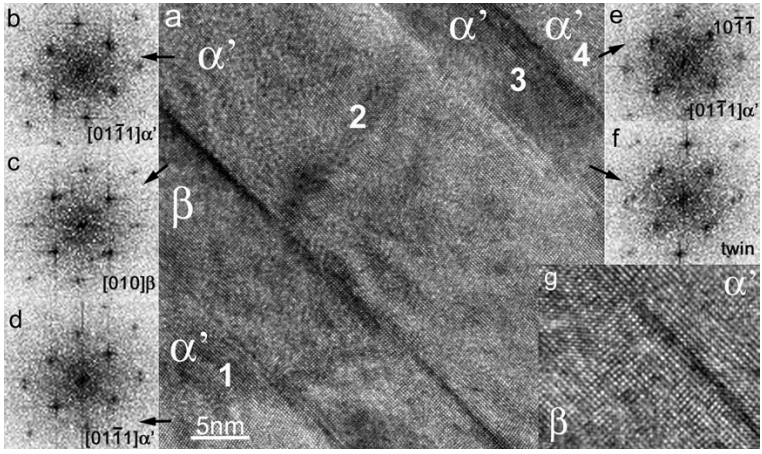

Figure 2. Microstructure of the as-quenched Ti-6Al-4V alloy after solution treatment at 1100°C. (a) HRTEM image of $\{10\bar{1}1\}$-type twin boundaries and α'/β interface. (b) to (f) show Fourier spectra of each crystal observed in (a). The crystals 1 and 2 have the same crystallographic orientation. A magnified image of the α'/β interface is shown in (g).

To examine possible formation of stacking faults at twin boundaries, we have carried out HRTEM observation on twin boundaries of an as-quenched Ti-6Al-4V alloy after solution treatment at 950°C. Figure 3a shows an HRTEM image of an as-quenched Ti-6Al-4V alloy after solution treatment at 950°C. The $\{10\bar{1}1\}$-type twin boundary is free from stacking faults or precipitates, in contrast to the case of the alloy solution treated at 1100°C shown in Figs.1 and 2. Such a clear twin boundary can be compared to that of observed in Ti-12mass%V-2mass%Al alloy with excellent ductility [8, 9]. Note that stacking faults or thin β plate was not found in this alloy after solution treatment at 950°C, which is lower than the β transus by 45K. Microstructure of this alloy composed of equiaxed α grains in addition to acicular α' martensites [7]. Figure 3b

shows another example of the $\{10\bar{1}1\}$ twin boundary with very thin stacking faults, composed of a few atomic layers. However, an attached SAED pattern obtained from an area including both twin boundaries shown in Figs.3a and 3b shows no streak, indicating the fact that the population of such a twin boundary including stacking fault is quite small.

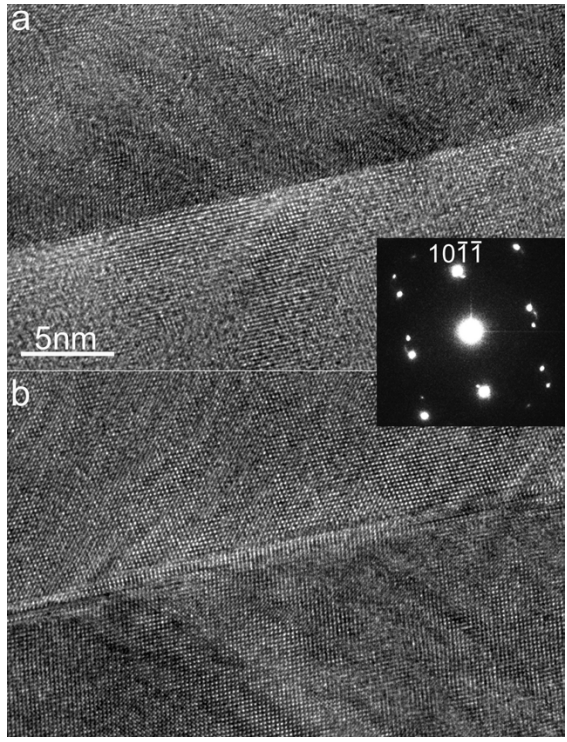

Figure 3 Twin boundary of the as-quenched Ti-6Al-4V alloy after solution treatment at 950°C. (a) HRTEM image of a twin boundary with no stacking faults or precipitates. (b) A twin boundary including very thin stacking faults, composed of only 2-3 atomic layers. Attached SAED pattern includes reflections related to the $\{10\bar{1}1\}$ twin, but the streak pattern is not seen along the twin axis.

According to the recent work [7], the as-quenched alloy solution treated at 1100°C is brittle, while the alloy solution treated at 950°C is ductile with higher strength. The latter alloy shows excellent cold rolling ability more than 40% [7]. The brittle fracture of the former alloy can be attributed to the stacking faults at the $\{10\bar{1}1\}$ twin boundary and/or thin β plate among the α' martensite plates. It is considered that these stacking faults and thin β layers are formed at the

quench after solution treatment, however, their origin including energetics is not clear at this moment.

Conclusion

AC-HRTEM observation revealed atomic structures of the $\{10\bar{1}1\}$-type twin boundary of two types of as-quenched Ti-6Al-4V alloys unambiguously. The alloy solution treated at 1100°C includes stacking faults at the twin boundary, which leads to brittle fracture. In contrast, the alloy solution treated at 950°C shows clear twin boundary mostly free from stacking faults or precipitates. The higher strength and ductility are observed in the latter alloy.

Acknowledgments

This work was partially supported by a Grant from the New Energy and Industrial Technology Development Organization (NEDO, 08E51003d). The high-resolution electron microscopy was carried out in the High-Voltage Electron Microscope Laboratory, Tohoku University.

References

1. E. W. Collings, *The Physical Metallurgy of Titanium Alloys* (ASM, Metals Park, Ohio, 1984).
2. G. Lutjering and J. C. Williams, *Titanium* (Springer, Berlin, 2003).
3. M. Niinomi, "Recent Metallic Materials for Biomedical Applications", *Metall. Mater. Trans. A*, 33 (3) (2002), 477-486.
4. P. Castany, F. Pettinari-Sturmel, J. Douin, and A. Coujou, "In Situ Transmission Electron Microscopy Deformation of the Titanium Alloy Ti-6Al-4V: Interface Behaviour", *Mater. Sci. Eng. A*, 483-484 (2008), 719-722.
5. H. Matsumoto, S. Watanabe, and S. Hanada, "α' Martensite Ti-V-Sn Alloys with Low Young's Modulus and High Strength", *Mater. Sci. Eng. A*, 448 (1-2) (2007), 39-48.
6. H. Matsumoto, A. Chiba, and S. Hanada, "Anisotropy of Young's Modulus and Tensile Properties in Cold Rolled α' Martensite Ti-V-Sn Alloys", *Mater. Sci. Eng. A* 486 (1-2) (2008), 503-510.
7. H. Matsumoto, H. Yoneda, K. Sato, S. Kurosu, E. Maire, D. Fabregue, A. Chiba, and T. J. Konno, "Room Temperature Ductility of Ti-6Al-4V Alloy with α' Martensite Microstructure", *Mater. Sci. Eng. A*, in press.
8. H. Matsumoto, K. Kodaira, K. Sato, T. J. Konno, and A. Chiba, "Microstructure and Mechanical Properties of α' Martensite Type Ti Alloys Deformed under the α' Processing", *Mater. Trans.*, 50 (12) (2009), 2744-2750.
9. K. Sato, H. Matsumoto, K. Kodaira, T. J. Konno, and A. Chiba, "Phase Transformation and Age-hardening of Hexagonal α' Martensite in Ti-12mass%V-2mass%Al Alloys Studied by Transmission Electron Microscopy", *J. Alloys Compd.*, 506 (2) (2010), 607-614.
10. H. Matsumoto, H. Yoneda, K. Sato, T. J. Konno, S. Kurosu, D. Fabregue, E. Maire, and A. Chiba, "Microstructure and Mechanical Properties of α' Martensite Type Ti-V-Al Alloy after Cold- or Hot Working Process", *Key Eng. Mater.* 436 (2010), 171-177.
11. E. W. Collings, *Material Properties Handbook, Titanium Alloys*, ed. R. Boyer, G. Welsch, and E. W. Collings (ASM International, Ohio, USA, 1994), 490.